An innovative application of ($Ni_X Zn_X$–X Fe_2O_4) Mineral nanoparticles for adsorption of Malachite green dye from wastewater effluents

M.R. Heydartaemeh

President & CEO at NanoMineTech Co., Tehran, Iran

Abstract

In this research work, the Ni-Zn Ferrite Mineral Nanoparticles (NZFMN), as a novel nanoadsorbent, was used for the removal of the Green Malachite (GM) dye from aqueous solutions by in a batch and fixed bed column. Firstly, the NZFMN adsorption properties were investigated. The effects of the process parameters including the contact time, adsorbent dosage, solution pH, and GM initial concentration were also studied. Thence, GM was quantitatively evaluated using the Freundlich and Langmuir isotherms and the pseudo-first- and second-order models. The adsorption data for the adsorption equilibrium was found to be described well using the Freundlich isotherm model. The results obtained for the AFM and SEM analyses showed that the particle size was less than 100 nm. Also the BET analysis showed that the surface area for NZFMN was 120 m^2/g. The results obtained also showed that the adsorption capacity and removal percentage of GM on NZFMN from wastewater was about 90%. Consequently, NZFMN was found to be a good adsorbent for wastewater purification.

Keywords: *($Ni_X Zn_X$–X Fe_2O_4) Mineral Nanoparticles, Green Malachite Dye, Adsorption, Wastewater Treatment.*

1. Introduction

Various colorants (dyes and pigments) are being applied in many industries for different coating applications. It is the inevitable reason for the existence of these materials in industrial wastewaters. Colored wastewaters, especially the organic ones, are wastes of different industries such as paper, textile, leather, food, polymers, minerals, and plastics [1]. The development of cost-effective and stable methods by nanomaterials for providing fresh water in adequate amounts is the need of the water industry. Thus treatment of water and wastewater contaminated with colorants is one of the main concerns of the researchers in the recent decades. In a real wastewater, there are different materials such as colorants, polyacrylates, phosphonates, and anti-coagulation factors. Most of these compounds are poisoning, and it is necessary for ecological balances that these dangerous contaminants are being removed completely from treated wastewaters. Therefore, the governments and different UN organizations have recently established many rules to prevent and standardize these materials in the environment [2, 3]. In the recent years, different physico-chemical decolorization processes such as reduction and precipitation [4], coagulation and flotation [5] membrane technologies and electrolysis [6, 7], biological treatments [8], advanced oxidation processes [9], chemical and electrochemical techniques [10, 11], and adsorption procedures [12-15] have been developed to remove contaminants from industrial wastewaters. Among all the treatments proposed, adsorption using sorbents is one of the most popular methods. It is now recognized as an effective, efficient, and economic method for water decontamination applications, and for the separation and analytical purposes [16].

However, most of these methods are expensive, and a certain economical foundation is necessary. Among the physico-chemical processes, the adsorption technology has found many applications in water and wastewater treatments, as one of the most efficient and effective technologies [2, 17]. Therefore, natural adsorbents such as diatomite [2], red mud [18], chitosan [19], orange skin [20], soy meal hull [21], almond skin [22], sawdust [23], zeolite [24], clay [25], carbon [26], and diatomite–perlite composite [27] have been used to reduce costs and the environmental side-effects. These adsorbents have a natural base, and they are environmentally friendly. It is possible to regenerate most of them or apply them in different products.

The nanometer material is a new functional material that has attracted much attention due to its special properties. Most of the atoms on the surface of nanoparticles (NPs) are unsaturated and can easily bind to other atoms. NPs have a high adsorption capacity. Besides, the operation is simple, and the adsorption process is rapid. Thus there is a growing interest in the application of NPs as adsorbents [28-30].

Adsorption isotherms describe how adsorbents interact with adsorbents. Adsorption isotherms demonstrate the relationships between equilibrium concentrations of adsorbate in the solid phase (q) and in the liquid phase (C) at a constant temperature [22, 31, 32]. Adsorption isotherms are described in many mathematical forms. They are often obtained in the laboratory using the batch test, in which the equilibrium data is attempted by various isotherm models such as the Langmuir and Freundlich isotherms [33-36]. The Langmuir isotherm model suggests that the uptake of adsorbate occurs on the homogeneous surface by monolayer sorption without interaction between the adsorbed molecules. The model assumes that the energies of adsorption on the surface are uniform and no migration of adsorbate happens on it. The linear form of the Langmuir isotherm equation is represented by the following equation [37]:

$$\frac{C_e}{q_e} = \frac{1}{QK_L} + \frac{C_e}{Q} \tag{1}$$

where C_e is the equilibrium concentration of the adsorbate (mg/L), q_e is the amount of adsorbed GM at equilibrium (mg/g), and Q (mg/g) and K_L (L/mg) are the Langmuir constants related to the adsorption capacity and energy, respectively. When C_e/q_e is plotted against C_e, a straight line is

obtained with the slope $1/Q$ and the intercept $1/QK_L$. It shows that the adsorption of GM follows the Langmuir parameters.

The Freundlich equation has been widely used and it is applicable to isothermal adsorption. This model is a special case for heterogeneous surface energies in the Langmuir equation. In this model, the energy term varies as a function of the surface coverage, q_e, which strictly depends upon the variations in the heats of adsorption [36, 38]. The Freundlich equation has the following general form [22, 39]:

$$log\, q_e = log\, K_F + (1/n) log\, C_e \tag{2}$$

where q_e is the amount of adsorbed GM per until weight (mg/g adsorbent), C_e is the equilibrium concentration of the adsorbate (mg/L), and K_F and n are the Freundlich constants.

It is essential to predict the rate at which the dye is removed from aqueous solutions in order to design an appropriate treatment system based on the adsorption process. The pseudo-first- and pseudo-second-order models have been applied to describe the adsorption kinetics of GM by NZFMN. The pseudo-first-order kinetics model can be represented by the following Lagergren's expression:

$$\ell n\,(q_e - q_t) = \ell n\,q_e - K_{1,ad}\,(t) \tag{3}$$

where q_e and q_t are the amounts of dye adsorbed (mg/g) at equilibrium and at time t (min), respectively, and $K_{1,ad}$ is the pseudo-first-order rate constant (1/min). The rate of pseudo-second-order model depends upon the amount of dye adsorbed on the surface of the adsorbent and its quantity in the equilibrium condition [39]. The pseudo-first-order model can be given as follows [40]:

$$\frac{1}{q_t} = \frac{1}{K_{2,ad}\,q_e^2\,t} + \frac{1}{q_e} \tag{4}$$

2. Experimental studies (materials and equipment)

Nowadays, with the help of new methods such as magnetization, the efficiency of natural adsorbents for adsorption of pollutants from aqueous solutions has slightly decreased [29, 30] but the adsorbent can be easily separated from a mixture of particles using a simple magnet. Thus in this research work, the removal of GM from simulated textile wastewater was investigated by NZFMN. The Ni-Zn ferrite mineral is a natural and cheap adsorbent. Thus the Ni-Zn ferrite mineral

nanoscale size of this adsorbent was prepared by a mill (EQ‑PC‑12 model).

The objective of the present work was to focus on the development of NZFMN for the removal of GM. The dye selected in this work was MG due to its environmental significance. The effects of adsorbent dosage, contact time, solution pH, and GM initial concentration were investigated. Characterization of the isothermal adsorption and adsorption kinetics and also the AFM, SEM, and BET analyses were studied in order to provide a new method and theoretical evidences for wastewater treatment.

The ($Ni_X Zn_X$–X Fe_2O_4) mineral NPs used in this investigation as a novel adsorbent was obtained from the NanoMineTech Company (a source in Iran); it could be prepared from any material construction store. GM was supplied from the Ciba Company; its molecular structure is shown in Figure 1.
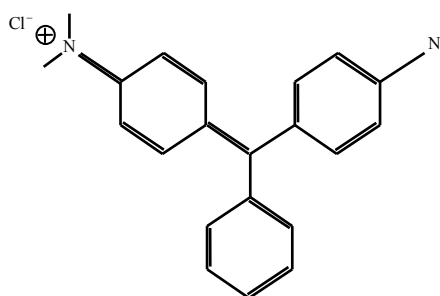
Figure 1. Molecular structure of GM pigment.

A laboratory scale (Sartorius-d = 0.1 mg, max 120 g model) was used to weigh the samples. Some simple laboratory heater-stirrer systems were used to mix the samples. A UV/visible spectrometer (one-beam) was used to measure the change in concentration of GM, and a high-temperature oven (1100°) (Cecil-CE2021-2000 series) was used for drying. In addition, various sieves with different meshes were used to categorize the adsorbent. A centrifuge (Hettich EBA20, maximum whirl = 6000 rpm) was used to sediment and remove the colloidal particles, and a pH-meter (Metrohm 713) was used to measure and adjust the pH of simulated wastewater. A mill (EQ-PC1-12) that crushed particles, a spray dryer (BUCHI B-191) for drying slurry particles, a SEM

(Scanning Electron Microscope, LEO 1455VP), an AFM (Atomic Force Microscope, Model SZMU-L5), and BET analysis were used to increase the knowledge about the NZFMN microscopic structure and its real nature. The other chemicals used including sodium hydroxide and chloridric acid were supplied from Merck Company, especially to adjust the pH of wastewater.

2.1. Adsorption procedure

The adsorption measurements were conducted by mixing various amounts of the $Ni_X Zn_X$–X Fe_2O_4 mineral NPs (0.05 g) in a stirrer containing a GM dye solution (6, 8, 12, 20 ppm) at 25 °C and pH=6 for 120 min to attain the equilibrium condition. The mixing rate was high enough (>3000 rpm) to minimize the external mass transfer resistance. The adsorption changes were determined at certain times (0, 10, 30, 60, 90, and 120 min) during the removal process. After conducting the adsorption experiment, the solution was separated from NZFMN by centrifugation at 4000 rpm for 5 min using a Hettich EBA20 centrifuge. The percentage adsorption of the dye from its aqueous solution was computed as follows:

$$\text{Adsorption}\,(\%) = \frac{C_{int} - C_{fin}}{C_{int}} \times 100 \tag{5}$$

where C_{int} and C_{fin} are the initial and final dye concentrations, respectively. The dye concentrations in the aqueous solution were determined using a CECIL 2021 spectrophotometer corresponding to the maximum wavelength ($\lambda_{max} = 619\,\text{nm}$) for MG.

2.2. X-ray diffraction

The chemical constituent of NZFMN, as the adsorbent, for GM was calculated by the X-Ray Diffraction (XRD) method using a Philips X-Ray Diffractometer Xunique 1140; it was done to characterize the minerals existing in the NZFMN phase, is the major phase is the spinel phase ($Ni_X Zn_X$–X Fe_2O_4) and ferrite phase with space Fd^3m group at the samples in Figure 2.
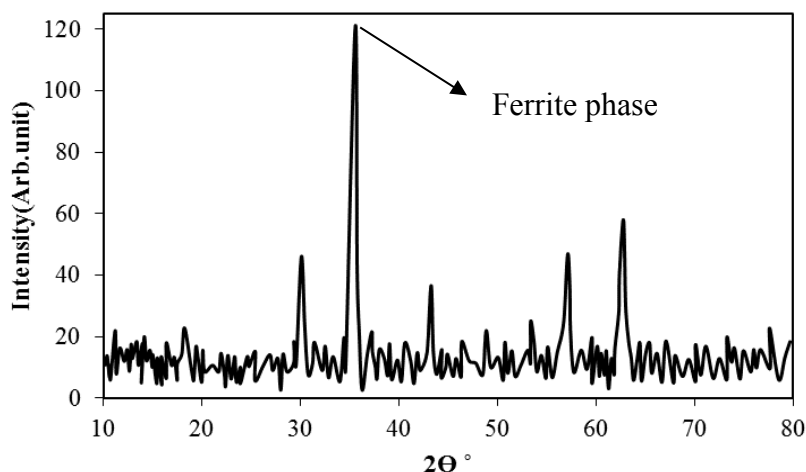
Figure 2. XRD patterns for NZFMN samples.

2.3. TEM analysis of NZFMN sample

The transmission electron microscopy (TEM) patterns for NZFMN are shown in Figure 3. As shown, the particle size of the NZFMN sample was about 50 nm.

One of the low-cost minerals is NZFMN, which is abundant in many countries such as Iran (west and NW Iran). It typically exhibits a dark color. This volcanic rock has an extremely porous structure with a large surface area. NZFMN has been found to be effective due to its high porosity and structure, large surface area, negatively charged surface, low cost, and natural ability.
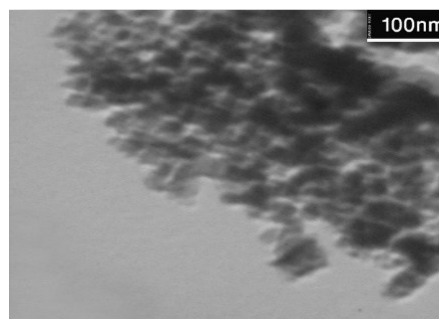

Figure 3. TEM image for NZFMN samples.

Adsorbent	Metal ions/MG dye	Maximum adsorption capacity (mg/g)	Source
NZFMN	MG Dye	90	Present study
Montmorillonite	Ni^{2+}	12.886	
Pumice	Cu^{2+}	0.055 (mmol/g)	
Kaolinite	Cd^{2+}	9.9	
Bentonite	Cd^{2+}	9.3	
Montmorillonite	Cd^{2+}	6.784	
Scolecite	Cd^{2+}	0.0078 (meq/g)	
Bigadic clinoptilolite	Cd^{2+}	0.0053 (meq/g)	
Montmorillonite	Pb^{2+}	0.68	
Kaolinite	Pb^{2+}	0.12	
Zeolite	Cu^{2+}	141.12	
Vermiculite	Cd^{2+}	143 (µmol/g)	
Diatomite	Pb^{2+}	24.94	
Perlite	Pb^{2+}	8.906	

3. Results and discussion
3.1. Effect of pH

Solution pH is an important factor that controls an adsorption process. The effect of pH on the MG adsorption by NZFMN was investigated in the pH values 4, 6, and 8. Figure 4 shows the MG adsorption percentage as a function of pH and contact time. As it is shown in this figure, the dye adsorption fall with an increase in the solution pH. The maximum GM removal took place at pH = 6, and the slope was closer to the equilibrium after 120 minutes.
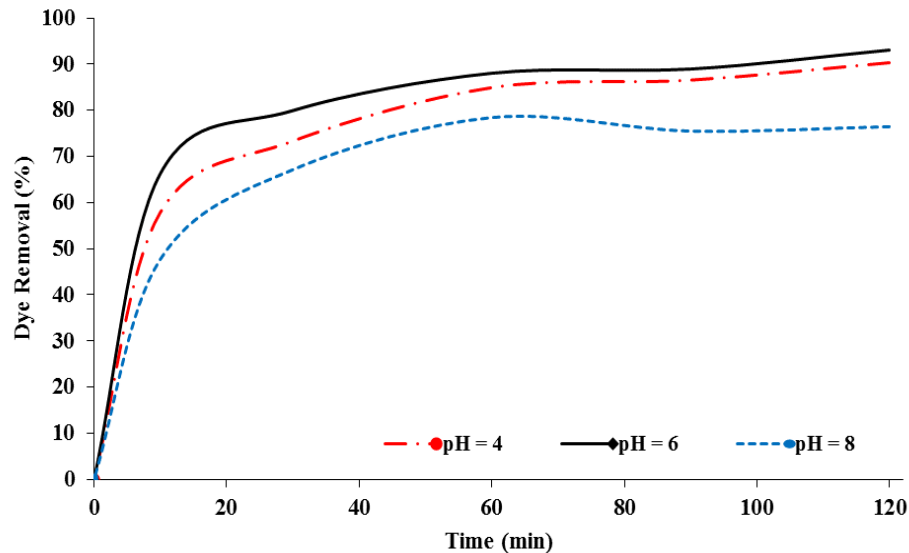
Figure 4. Effect of pH on adsorption of GM by NZFMN.

3.2. Effects of (Ni$_X$Zn$_X$–X Fe$_2$O$_4$) mineral NP dosage and contact time

In the non-linear adsorption case, there exists a good fitting between the numerical model and the laboratory breakthrough curves. According to the results obtained, the increased contact time between the adsorbent and GM from aqueous solutions flow in the system, and accordingly, the adsorbent was saturated faster on the hydrogen bonded O–H groups in curves. The effect of the NZFMN dosage on the GM removal, which was based upon the contact time, was studied by changing the adsorbent dosage in the range of 0.01, 0.03, 0.05, and 0.07 g. The results obtained are presented in Figure 5.

Based on this figure, the removal trend of GM from 20 ppm of simulated wastewater was done at pH = 6 by 0.01 g, 0.03 g, 0.05 g, and 0.07g per 25 mL of solution. The dosages 20 ppm and 0.07 g of NZFMN had the most effective adsorption values. Additionally, the adsorption yield increased with contact time and attained a maximum value at 120 min. Applying more adsorbent than the optimized dosage (0.07 g) diminished the capacity of the adsorption process.
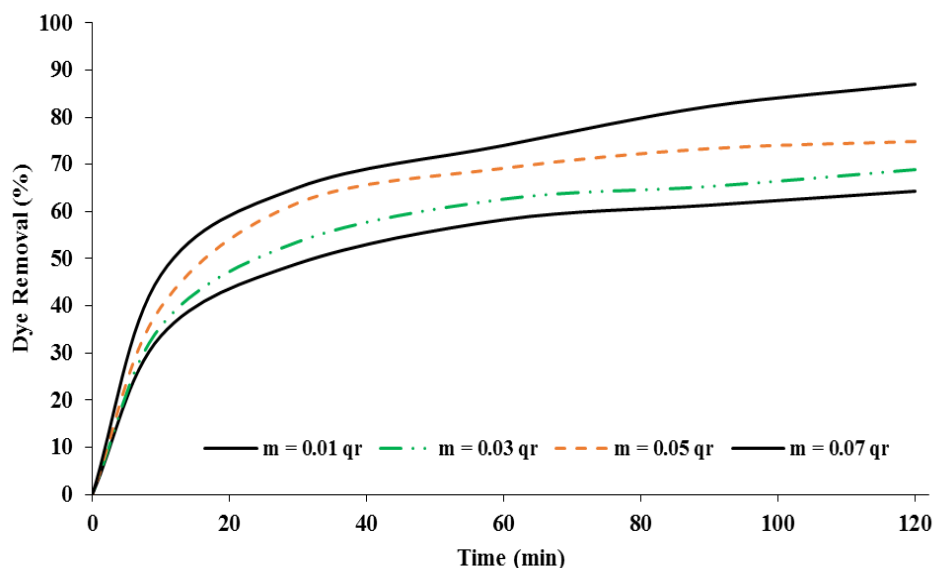

Figure 5. Effect of NZFMN dosage on GM adsorption.

147

3.3. Effect of initial GM concentration

The effect of the initial GM concentration on the adsorption process was investigated by changing the initial dye concentration in the range of 6, 8, 12, and 20 ppm under the optimized conditions (pH = 6, contact time of 120 min, adsorbent dosage of 20 ppm, and environmental temperature). The GM adsorption efficiency decreased with increase in the initial dye concentration. When the GM concentration increased from 6 to 20 ppm, the adsorption percentage increased (Figure 6).
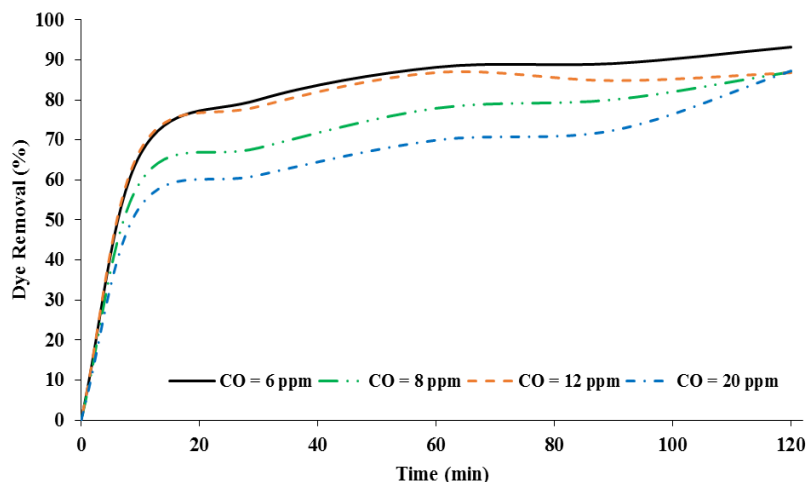

Figure 6. Effect of GM initial concentration on adsorption by NZFMN.

3.4. FT-IR analysis

In order to identify the surface characteristics and functional groups of the ($Ni_XZn_X–X$ Fe_2O_4) mineral NPs, FT-IR analysis was performed in the range of 450-4000 cm^{-1} in the Central Laboratory of Amirkabir University of Technology (Figure 7). The broad absorption band at 3443.71 cm^{-1} can be attributed to the stretching vibration of the hydrogen bonded O–H groups, and the absorption band at 2920–2955 cm^{-1} can be related to the stretching vibration mode of the C-H group. Also we have two main broad metal–oxygen bands, which can be assigned to the spinel phase. The lowest band, usually observed in the range of 450–385 cm^{-1}, can be assigned to the octahedral-metal stretching, and the strongest one appearing in the 600–550 cm^{-1} range corresponds to the intrinsic stretching vibrations of the metal at the tetrahedral site. As it can be seen in this spectrum, the broad band in 558.5 cm^{-1} is an indication of the ferrite phase formation.
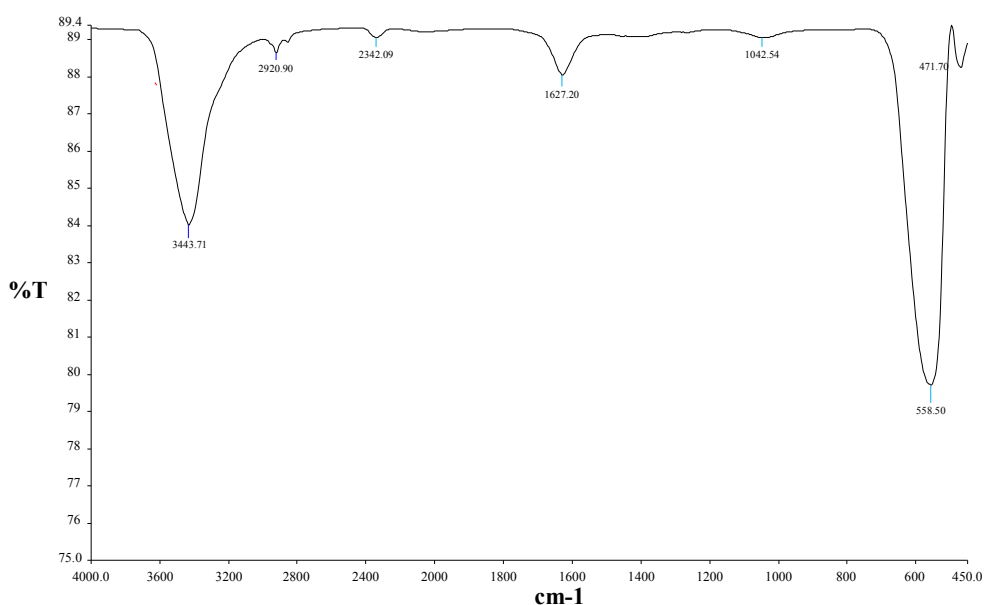

Figure 7. Results of FT-IR analysis of NZFMN samples.

3.5. SEM analysis of NZFMN samples

The images of the NZFMN surfaces were obtained using a SEM instrument, model LEO 1455VP, which illustrated raw NZFMN by zooming low (Figure 8a) and more zoom for the $(Ni_X Zn_X–X\ Fe_2O_4)$ mineral NPs before (Figure 8b) and after GM adsorption (Figure 8c). This characteristic causes NZFMN to be a proper adsorbent. Moreover, comparison of figures 8b and 8c shows that the nanosurfaces were treated and prepared to adsorb pollutants from the wastewater, and that the structure of the surface of NZFMN completely changed before and after the process. The extra parts and porosity were removed.

3.6. AFM and BET analysis of NZFMN samples

Atomic force microscopy (AFM) is a powerful tool allowing a variety of surfaces to be imaged and characterized at the atomic level. According to Figure 9, NZFMN, as a nanoadsorbent, has a high porosity, and this porosity, as an effective factor, has an important role in the GM adsorption. The result of the BET analysis for the surface area of NZFMN was 120 m^2/g.

3.7. Adsorption isotherms

The empirical parameters for the $(Ni_X Zn_X–X\ Fe_2O_4)$ mineral NPs are given in Table 1. The fitting of the experimental data in each isotherm model was examined by calculation of the correlation factor (R^2). The Freundlich model was found to better describe the adsorption than the Langmuir model according to the correlation factor $(R^2 = 1.0)$. As it can be seen in this table, the highest R^2 values for the Freundlich model show that it is the most suitable equation to describe the adsorption equilibrium. According to this model, the Freundlich constants K_f and n were calculated to be 7.1345 and 2.997, respectively, for NZFMN. These are relatively uncommon but are often observed at low concentration ranges for compounds containing a polar functional group. Consequently, the GM adsorption by NZFMN follows the Freundlich isotherm model.

3.8. Adsorption kinetics

Where $K_{2,ad}$ is the rate constant of the pseudo-second-order model (g/mg min), the kinetics parameters of the pseudo-first-order and pseudo-second-order models of GM at different pH values and temperatures are given in Tables 1 and 2.

Tables 1 and 2 explain that the adsorption kinetics of GM by the adsorbent can be well-described by the pseudo-second-order reaction model at various pH values and temperatures.
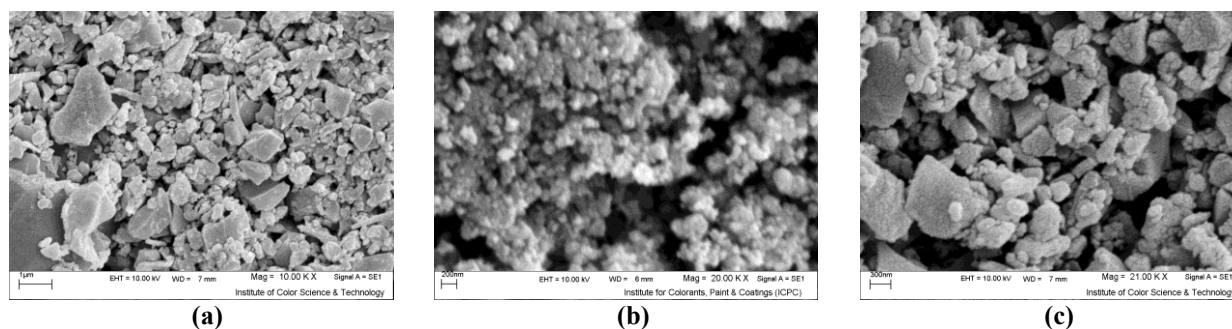

(a)	(b)	(c)

Figure 8. SEM images for external surface of raw NZFMN by zooming low (a) and more zoom for NZFMN before (b) and after adsorption process (c).
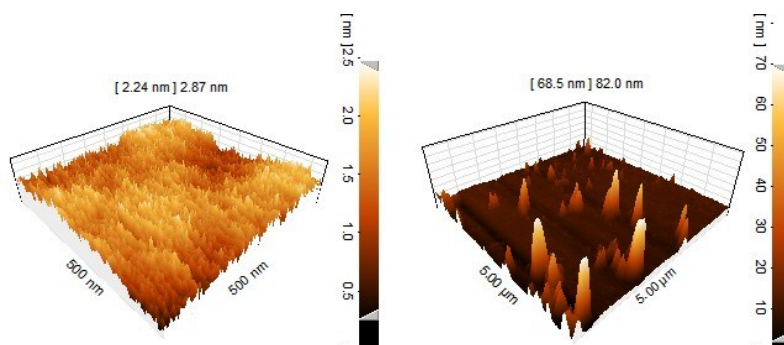

Figure 9. AFM image of NZFMN obtained in wet cell.

Table 1. Isotherm coefficients for adsorption of GM on NZFMN.

Adsorbent type	Langmuir isotherm			Freundlich isotherm		
	Q	K_L	R_2^2	K_F	n	R_1^2
$(Ni_X Zn_X - X\ Fe_2O_4)$ mineral Nanoparticles	67	0.238	**0.927**	7.1345	2.997	**0.998**

Table 2. Kinetics constants for GM obtained at pH = 4, 6, and 8.

pH	Pseudo-first-order		Pseudo-second-order	
	$K_{1,ad}$	R^2	$K_{2,ad}$	R^2
4	0.0039	0.5328	0.0007	0.4683
6	0.0091	0.794	0.003	0.893
8	0.0073	0.6735	0.0034	0.693

4. Conclusions

The SEM and AFM results of this research work showed that the surface morphology of $(Ni_X Zn_X - X\ Fe_2O_4)$ mineral NPs had a very important role in the adsorption process in low bulk mass transfer velocity (rotational speed of stirrer). Since NZFMN was prepared from Ni-Zn ferrite mineral NPs, as a natural adsorbent, it is a novel low-price adsorbent. NZFMN was applied to remove GM from a simulated wastewater. The GM adsorption by NZFMN depends upon different parameters such as particle size, pH, adsorbent dosage, and temperature. The maximum percentage of GM removal was about 90%, which was obtained in the normal temperature (25 °C) and at pH = 6. The results of fixed bed column showed that 6, 8, and 10 mL/min flow rates the break through curve were saturated in 150, 300, and 450 min, respectively. The fitting of the experimental data in each isotherm model was examined by calculation of the correlation factor (R^2). It was found that the Freundlich model better described the adsorption than the Langmuir model, according to the correlation factor ($R^2 = 1.0$). As it could be seen in Table 1, the highest R^2 values for the Freundlich model showed that it was the most suitable equation to describe the adsorption equilibrium. Based upon the results obtained, the Freundlich model better described the adsorption than the Langmuir model. It was essential to predict the rate at which the dye was removed from aqueous solutions in order to design an appropriate treatment system based on the adsorption process. The pseudo-first- and pseudo-second-order models were applied to describe the adsorption kinetics of GM by NZFMN. The adsorption kinetics of GM by the NZFMN adsorbent could be well described by the pseudo-second-order reaction model at various pH values.

References

[1]. Erdem, E., Çölgeçen, G. and Donat, R. (2005). The removal of textile dyes by diatomite earth. Journal of Colloid and Interface Science. 282 (2): 314-319.

[2]. Saberi, M., Kor, M., Badii, K.H. and Yousefi Limaee, N. (2009). Applying the Taguchi experimental design method to optimize the dyes removal from simulated wastewater by diatomite. In English Proceedings of International Conference on Water Resources ICWR. pp. 566-573.

[3]. Al-Ghouti, M.A., Khraisheh, M.A.M., Allen, S.J. and Ahmad, M.N. (2003). The removal of dyes from textile wastewater: a study of the physical characteristics and adsorption mechanisms of diatomaceous earth. Journal of Environmental Management. 69 (3): 229-238.

[4]. Esalah, J.O., Weber, M.E. and Vera, J.H. (2000). Removal of lead, cadmium and zinc from aqueous solutions by precipitation with sodium Di-(n-octyl) phosphinate. The Canadian Journal of Chemical Engineering. 78 (5): 948-954.

[5]. Zouboulis, A.I., Matis, K.A., Lanara, B.G. and Loos-Neskovic, C. (1997). Removal of cadmium from dilute solutions by hydroxyapatite. II. Flotation studies. Separation Science and Technology. 32 (10): 1755-1767.

[6]. Canet, L., Ilpide, M. and Seta, P. (2002). Efficient facilitated transport of lead, cadmium, zinc, and silver across a flat-sheet-supported liquid membrane mediated by lasalocid A. Separation Science and Technology. 37 (8): 1851-1860.

[7]. Ning, R.Y. (2002). Arsenic removal by reverse osmosis. Desalination. 143 (3): 237-241.

[8]. McMullan, G., Meehan, C., Conneely, A., Kirby, N., Robinson, T., Nigam, P., Banat, I., Marchant, R. and Smyth, W.F. (2001). Microbial decolourisation and

degradation of textile dyes. Applied microbiology and biotechnology. 56 (1-2): 81-87.

[9]. Lee, J.M., Kim, M.S., Hwang, B., Bae, W. and Kim, B.W. (2003). Photodegradation of acid red 114 dissolved using a photo-Fenton process with TiO2. Dyes and Pigments. 56 (1): 59-67.

[10]. Von Gunten, U. (2003). Ozonation of drinking water: Part I. Oxidation kinetics and product formation. Water research. 37 (7): 1443-1467.

[11]. Chen, X., Chen, G. and Yue, P.L. (2002). Novel electrode system for electroflotation of wastewater. Environmental science & technology. 36 (4): 778-783.

[12]. Ravindran, V., Stevens, M.R., Badriyha, B.N. and Pirbazari, M. (1999). Modeling the sorption of toxic metals on chelant-impregnated adsorbent. AIChE journal. 45 (5): 1135-1146.

[13]. Toles, C.A. and Marshall, W.E. (2002). Copper ion removal by almond shell carbons and commercial carbons: batch and column studies. Separation science and technology. 37 (10): 2369-2383.

[14]. Hu, Z., Lei, L., Li, Y. and Ni, Y. (2003). Chromium adsorption on high-performance activated carbons from aqueous solution. Separation and Purification Technology. 31 (1): 13-18.

[15]. Varma, A.J., Deshpande, S.V. and Kennedy, J.F. (2004). Metal complexation by chitosan and its derivatives: a review. Carbohydrate Polymers. 55 (1): 77-93.

[16]. Niu, C., Wu, W., Wang, Z., Li, S. and Wang, J. (2007). Adsorption of heavy metal ions from aqueous solution by crosslinked carboxymethyl konjac glucomannan. Journal of hazardous materials. 141 (1): 209-214.

[17]. Ramakrishna, K.R. and Viraraghavan, T. (1997). Dye removal using low cost adsorbents. Water Science and Technology. 36 (2-3): 189-196.

[18]. Badii, K., Doulati Ardejani, F. and Norouzi, S. (2009). Activation of alumina industrial waste for environmental purposes. In Proceedings of Iran International Aluminum Conference. Tehran IR Iran IIAC. pp. 592-595.

[19]. Chen, A.H., Liu, S.C., Chen, C.Y. and Chen, C.Y. (2008). Comparative adsorption of Cu (II), Zn (II), and Pb (II) ions in aqueous solution on the crosslinked chitosan with epichlorohydrin. Journal of Hazardous materials. 154 (1): 184-191.

[20]. Badii, K., Shafaie Tonekaboni, S.Z., Tehrani Bagha, A.R. and Yousefi Limaee, N. (2004). Optimization of condition of decolorization form wastewater containing direct dyes with using orange pills by Taguchi's experimental design method. In Proceedings of 1st Seminar on Environment and Color Tehran Iran ICPC. pp. 13-26.

[21]. Badii, K., Doulati Ardejani, F. and Yousefi Limaee, N. (2008). A numerical finite element model for the removal of direct dyes from aqueous solution by soy meal hull: optimization and sensitivity analysis. In First Conference and Workshop on Mathematical Chemistry Tarbiat Modares University Tehran Iran. pp. 57-64.

[22]. Ardejani, F.D., Badii, K., Limaee, N.Y., Shafaei, S.Z. and Mirhabibi, A.R. (2008). Adsorption of Direct Red 80 dye from aqueous solution onto almond shells: Effect of pH, initial concentration and shell type. Journal of hazardous materials. 151 (2): 730-737.

[23]. Bulut, Y. and Zeki, T.E.Z. (2007). Removal of heavy metals from aqueous solution by sawdust adsorption. Journal of Environmental Sciences. 19 (2): 160-166.

[24]. Chunfeng, W., Jiansheng, L., Lianjun, W., Xiuyun, S. and Huang, J. (2009). Adsorption of dye from wastewater by zeolites synthesized from fly ash: kinetic and equilibrium studies. Chinese Journal of Chemical Engineering. 17 (3): 513-521.

[25]. Gürses, A., Doğar, Ç., Yalçın, M., Açıkyıldız, M., Bayrak, R. and Karaca, S. (2006). The adsorption kinetics of the cationic dye, methylene blue, onto clay. Journal of Hazardous Materials. 131 (1): 217-228.

[26]. Farahmand, E., Rezai, B., Ardejani, F.D. and Tonekaboni, S.Z. (2015). Kinetics, equilibrium, and thermodynamic studies of sulphate adsorption from aqueous solution using activated carbon derived from rice straw. Bulgarian Chemical Communications. 47: 72-81.

[27]. Seifpanahi Shabani, K.S., Ardejani, F.D., Badii, K. and Olya, M.E. (2017). Preparation and characterization of novel nano-mineral for the removal of several heavy metals from aqueous solution: Batch and continuous systems. Arabian Journal of Chemistry. 10: S3108-S3127.

[28]. Maria, L., Santos, A.L., Oliveira, P.C., Valle, A.S., Barud, H.S., Messaddeq, Y. and Ribeiro, S.J. (2010). Preparation and antibacterial activity of silver nanoparticles impregnated in bacterial cellulose. Polimeros. 20 (1): 72-77.

[29]. Hashemian, S. (2010). MnFe 2 O 4/bentonite nano composite as a novel magnetic material for adsorption of acid red 138. African Journal of Biotechnology. 9 (50): 8667-8671.

[30]. Martins, A., Mata, T.M., Gallios, G.P., Václavíková, M. and Stefusova, K. (2009). Modeling and simulation of heavy metals removal from drinking water by magnetic zeolite. In Water Treatment Technologies for the Removal of High-Toxicity Pollutants. Springer. Dordrecht. pp. 61-84.

[31]. Markovska, L., Meshko, V. and Noveski, V. (2001). Adsorption of basic dyes in a fixed bed

column. Korean Journal of Chemical Engineering. 18 (2): 190-195.

[32]. McCabe, W.L., Smith, J.C. and Harriott, P. (1993). Unit operations of chemical engineering New York: McGraw-Hill. Vol. 5. 154 P.

[33]. Muhamad, H., Doan, H. and Lohi, A. (2010). Batch and continuous fixed-bed column biosorption of Cd 2+ and Cu 2+. Chemical Engineering Journal. 158 (3): 369-377.

[34]. Nitzsche, O. and Vereecken, H. (2002). Modeling sorption and exchange processes in column experiments and large scale field studies. Mine Water and the Environment. 21 (1): 15-23.

[35]. Chakraborty, S., De, S., DasGupta, S. and Basu, J.K. (2005). Adsorption study for the removal of a basic dye: experimental and modeling. Chemosphere. 58 (8): 1079-1086.

[36]. Shawabkeh, R., Al-Harahsheh, A. and Al-Otoom, A. (2004). Copper and zinc sorption by treated oil shale ash. Separation and Purification Technology. 40 (3): 251-257.

[37]. Doyurum, S. and Celik, A. (2006). Pb2+ and Cd2+ removal from aqueous solution by olive cake. J Hazard Mater. 138 (1): 22-28

[38]. Adamson, A.W. (1967). Physical Chemistry of Surfaces 2nd edition. Inter science Publishers Inc. New York

[39]. Gücek, A., Şener, S., Bilgen, S. and Mazmancı, M.A. (2005). Adsorption and kinetic studies of cationic and anionic dyes on pyrophyllite from aqueous solutions. Journal of colloid and interface science. 286 (1): 53-60.

[40]. Ho, Y.S. and McKay, G. (1998). Kinetic models for the sorption of dye from aqueous solution by wood. Process Safety and Environmental Protection. 76 (2): 183-191.

کاربردی جدید و نوآورانه از نانو ذرات معدنی (Ni$_X$Zn$_X$-X Fe$_2$O$_4$) برای جذب رنگزای سبز مالاکیت از پساب‌های صنعتی

محمدرضا حیدرطائمه

مدیرعامل شرکت توسعه معادن نانو تک

نویسنده مسئول مکاتبات: m.heydartaeme@nanominetech.com

چکیده:

در این کار تحقیقاتی، نانو ذرات معدنی فریت- نیکل روی Ni-Zn (NZFMN) به عنوان یک نانو ذره جدید و نوآورانه، برای حذف رنگ مالاکیت سـبز (GM) از محلول‌های آبی در ستون و بستر ثابت استفاده شد. در ابتدا خواص جاذب NZFMN مورد بررسی قرار گرفت. در طـی فرآینـد پارامترهـا شـامل زمـان تماس، مقدار غلظت جاذب، pH محلول و غلظت اولیه GM نیز مورد بررسی قرار گرفت. از این رو در این کار تحقیقاتی برای حذف رنگ مالاکیـت سـبز (GM)، ایزوترم‌های Freundlich و Langmuir و مدل‌های شبه اول و دوم مرتبه به صورت کمّی ارزیابی شد. داده‌های جذب برای بررسی مکانیسم تعادل به خـوبی بـا استفاده از مدل ایزوترم فروندلیچ همسو شده و توصیف شد. نتایج به دست آمده از آنالیزهای میکروسکوپ‌های AFM و SEM نشان داد که انـدازه ذرات کمتـر از ۱۰۰ نانومتر است. همچنین تجزیه و تحلیل BET نشان داد که سطح ویژه نانو ذرات معدنی فریت- نیکل روی NZFMN ۱۲۰ مترمربع بر گرم است. نتایج بـه دست آمده نشان داد که ظرفیت جذب و درصد حذف رنگ مالاکیت سبز (GM) در NZFMN از پساب مورد تحقیق در حـدود ۹۰ درصـد بـود کـه در نتیجـه، NZFMN یک جاذب خوب برای تصفیه پساب بود.

کلمات کلیدی: نانو ذرات معدنی (NiXZnX-X Fe2O4)، رنگزای مالاکیت سبز، جذب، تصفیه پساب.